OXFORD JOURNAL
OF STUDENT
SCHOLARSHIP

Acoustic Envelope Analysis of a Running 3D-Printed PLA Gear Pair

Anoushkaa Upadhyay[1]
anoushkaau@gmail.com

ABSTRACT

3D-printed gears made from polylactic acid (PLA) are widely used in classroom kits and other low-cost mechanisms, but they wear during repeated use, and there is no convenient way to tell that a gear is changing without stopping and dismantling the system. This study asks a deliberately narrow question: whether a single-channel sound level recording, of the kind a phone-based sound meter produces, contains time-localized events that can be detected reproducibly. One 42-minute run of a battery-driven two-gear PLA assembly was logged as relative sound level against time at 9.51 Hz and analyzed in Python. Because that sampling rate restricts the analysis to frequencies below 4.76 Hz, and because the gear pair carries 100 and 40 teeth, the gear-meshing frequency lies outside the measured band for any motor speed above 7.1 rev/min. The measurement is therefore treated throughout as an envelope measurement, describing how loudness varies over time rather than the acoustics of the meshing teeth. The record divides into a loud opening segment and a stationary remainder 7.0 dB quieter; only the stationary segment is analyzed. Within it, four events exceed the detection threshold, at 1,454, 2,019, 2,127 and 2,180 s. The same four events are returned by every analysis band between 0.5 and 4.5 Hz and every threshold between 6 and 9 dB above the segment mean, and none of 500 phase-randomized surrogates with the same power spectrum produced any detection at all. The study does not establish that these events reflect gear damage.

INTRODUCTION

Polylactic acid is known for its ease of use, low cost, and availability (Sandanamsamy et al.; Farah et al.). These properties are made possible through its low thermal expansion and high tensile strength. PLA is therefore often printed into gears for use in small-scale mechanical systems (Liao et al.), which is most visible in educational settings, where it is used in toolkits and student projects. Such gears are porous, and PLA is subject to degradation and fatigue after repeated use, with a fatigue life that depends on how quickly it is loaded as well as on how heavily (Česnik and Slavič). In most systems this leads to sudden failure, which is an extra cost to the user and disrupts the application. Industrial steel gears benefit from established protocols to prevent this situation (International Organization for Standardization, ISO 6336-1; ISO 20816-9), but there is no equally accessible method for tracking the condition of lightweight 3D-printed polymer gears without taking the system apart.

One possible route is acoustic analysis of the vibration produced when gear teeth mesh, because surface irregularities alter the sound a gear pair produces, and an acoustic measurement does not require the system to be disassembled (Qu et al.; Feng et al.). Established implementations of this idea rely on instrumentation that resolves the meshing frequency and its sidebands. The present study asks what, if anything, survives when the instrument is a phone-based sound meter logging at roughly ten samples per second.

Two properties of that measurement set hard limits on what this study can claim, and both are stated here rather than left for the reader to discover. First, the recording is a sound level log sampled at 9.51 Hz, so the analysis is restricted to fluctuations below 4.76 Hz. It describes the envelope of the sound the system produces, not the meshing frequencies that conventional gear diagnostics use. Second, the study reports a single run, and the gear was not inspected afterwards, so no detected event can be matched to any physical change in the gear. The study therefore does not test for fatigue, and no result below should be read as evidence of fatigue.

What the paper does contribute is a documented and fully reproducible procedure for extracting time-localized events from a low-rate acoustic log, together with two tests of whether those events are properties of the signal or of the analyst's choices. The question it answers is whether such events can be detected at all, and how robustly, which is a precondition for any later study that attempts to connect them to gear condition.

METHODS

Apparatus and Recording

The gear pair was part of a 3D-printed educational kit, shown in Figure 1. A 40-tooth input gear and a 100-tooth output gear, both printed in PLA, were mounted on a perforated PLA baseplate so that their teeth meshed, giving a reduction ratio of 2.5 to 1. Tooth counts were confirmed from a photograph of the assembly by taking the Fourier transform of the gear outline radius as a function of angle; the dominant angular harmonics are 100 and 40. A small direct-current motor driven by two AA cells was fixed directly to the input gear, with no intermediate reduction stage. Sound was recorded with the built-in microphone of an Apple iPhone running the phyphox acoustic logging experiment, placed beside the assembly and left undisturbed for the duration; its distance from the gear pair was not recorded at the time, so absolute levels would not be comparable with another recording even if the instrument had been calibrated. The recording was made on 20 December 2025 between 18:28 and 19:10 local time, and ran for 2,528 s. The instrument calibration offset was zero, so levels are reported as relative decibels and no absolute sound pressure level is claimed. This paper reports one run; no second run exists, and the apparatus has since been dismantled.

Signal Conditioning and Segmentation

The exported file contained 24,044 rows, of which the final 832 carried no level value and were removed, leaving 23,212 samples spanning 0 to 2,440.6 s. The mean sample interval is 0.1051 s, giving a sampling rate of 9.51 Hz and, by the Nyquist criterion, an analysis limit of 4.76 Hz (Oppenheim and Schafer). Levels were converted from decibels to linear amplitude using linear amplitude = 10^(dB/20) before any frequency-domain step.

Inspection of the record showed that it is not stationary. The first 565 s sit 7.0 dB above the remainder, with a mean of -59.5 dB against -66.4 dB and a standard deviation of 3.6 dB against 2.7 dB. Because a detection threshold referred to the mean of a whole record is not meaningful when the record contains a step of this size, the opening segment was excluded and all subsequent analysis was performed on the stationary remainder, 565.3 to 2,440.6 s, a span of 31.3 minutes. The cause of the step was not recorded and is not identified here.

Frequency-Domain Analysis

The spectrum of the stationary segment was computed by Fourier transform of the linear amplitude signal, with magnitudes scaled by two divided by the number of samples. A spectrogram was then computed using a segment length of 512 samples with 256 samples of overlap, which at 9.51 Hz corresponds to a 53.8 s window advanced in 26.9 s steps, giving a frequency resolution of 0.019 Hz and a time resolution of 53.8 s. Any event located by this method is therefore localized to a window rather than to an instant.

Event Detection and Its Justification

Mean spectrogram power in the 1 to 3 Hz band was computed for each window, producing a single curve of band level against time, and events were taken as peaks in that curve exceeding the segment mean by 6 dB. Neither the band nor the threshold was derived from theory, so both were tested rather than asserted. The band was varied across 0.5 to 2, 1 to 2, 1 to 3, 2 to 4 and 0.5 to 4.5 Hz and the threshold across 3 to 9 dB above the segment mean, and the resulting event sets were compared. Separately, the detection procedure was run unchanged on 500 phase-randomized surrogates of the stationary segment. Each surrogate preserves the power spectrum of the measured signal exactly while destroying its time structure, so the number of detections a surrogate produces is the number this procedure returns from a stationary process with the same spectrum and no events in it. All processing used Python with NumPy (Harris et al.) and SciPy (Virtanen et al.).

RESULTS

The full record and the level step that divides it are shown in Figure 2. The step at 565 s is abrupt and separates a louder, more variable opening from a quieter remainder, and all four events reported below fall in the second half of the stationary segment.

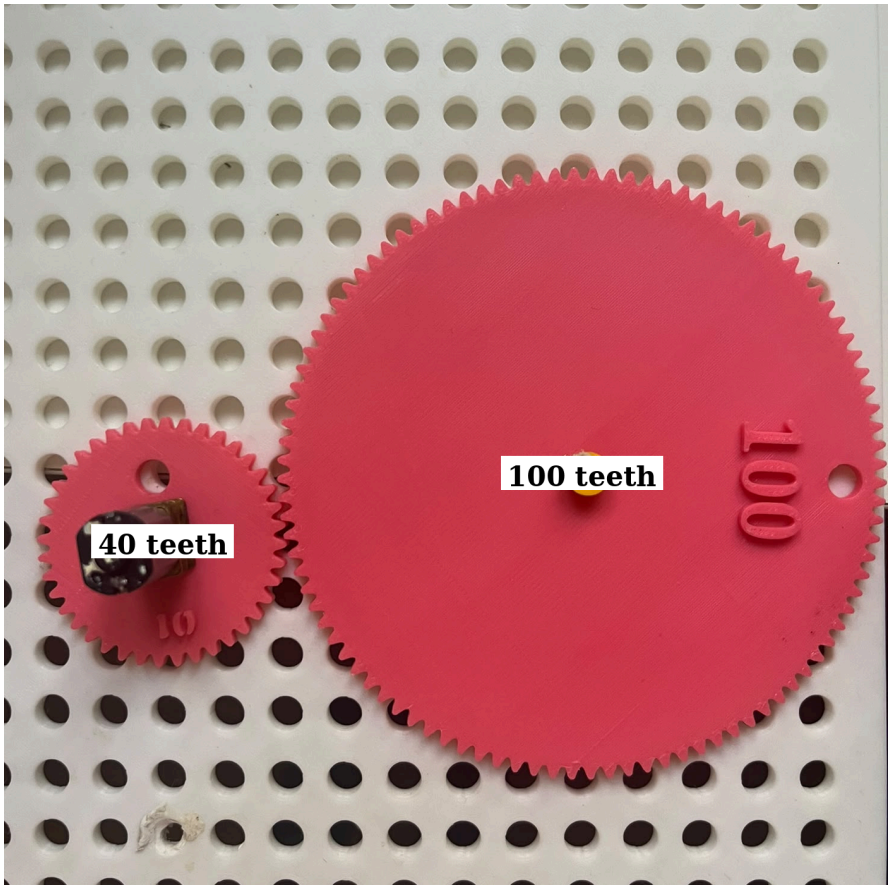


Figure 1. The gear assembly. A 40-tooth PLA input gear, driven directly by a two-cell direct-current motor, meshes with a 100-tooth PLA output gear on a perforated PLA baseplate. Tooth counts were measured from this photograph by Fourier analysis of each gear outline. The reduction ratio is 2.5 to 1.

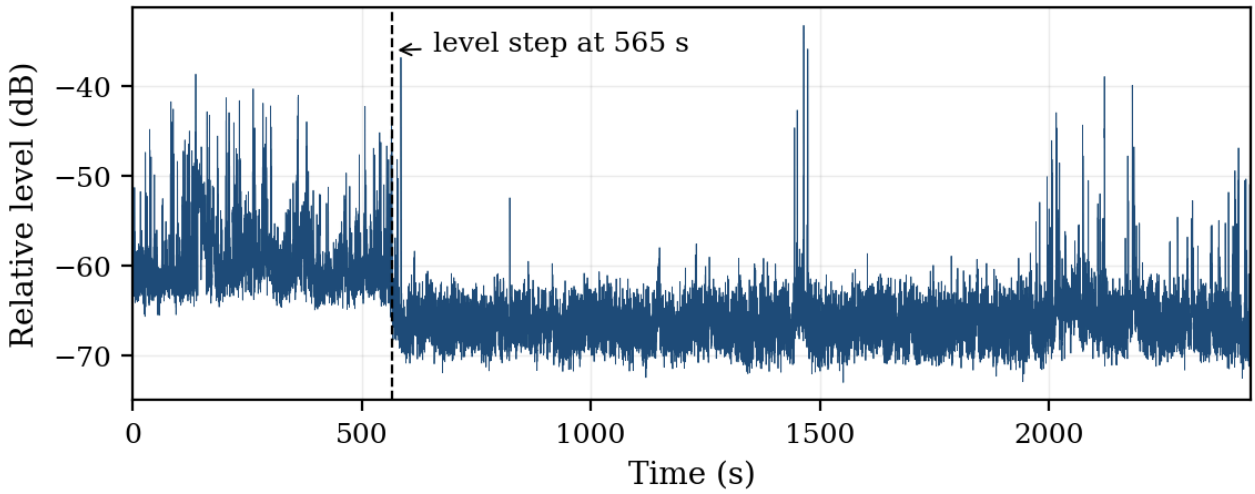


Figure 2. Relative sound level across the full 2,441 s record, after removal of 832 rows with missing values. The dashed line at 565 s marks an abrupt 7.0 dB step: the opening segment has a mean of -59.5 dB and a standard deviation of 3.6 dB, the remainder -66.4 dB and 2.7 dB. Only the segment to the right of the dashed line is analyzed in this paper.

Within the stationary segment, spectral energy falls monotonically with frequency across the measured range and shows no discrete line (Figure 3). The spectral centroid is 1.68 Hz and the spectral spread is 1.36 Hz, and the 1 to 3 Hz band carries 38.3 percent of the total magnitude below 4.76 Hz. Computed separately over four equal blocks of the stationary segment, the centroid is 1.70 Hz with a standard deviation of 0.11 Hz and the spread is 1.40 Hz with a standard deviation of 0.06 Hz, so the spectral description of the signal is stable to about 6 percent across the segment.

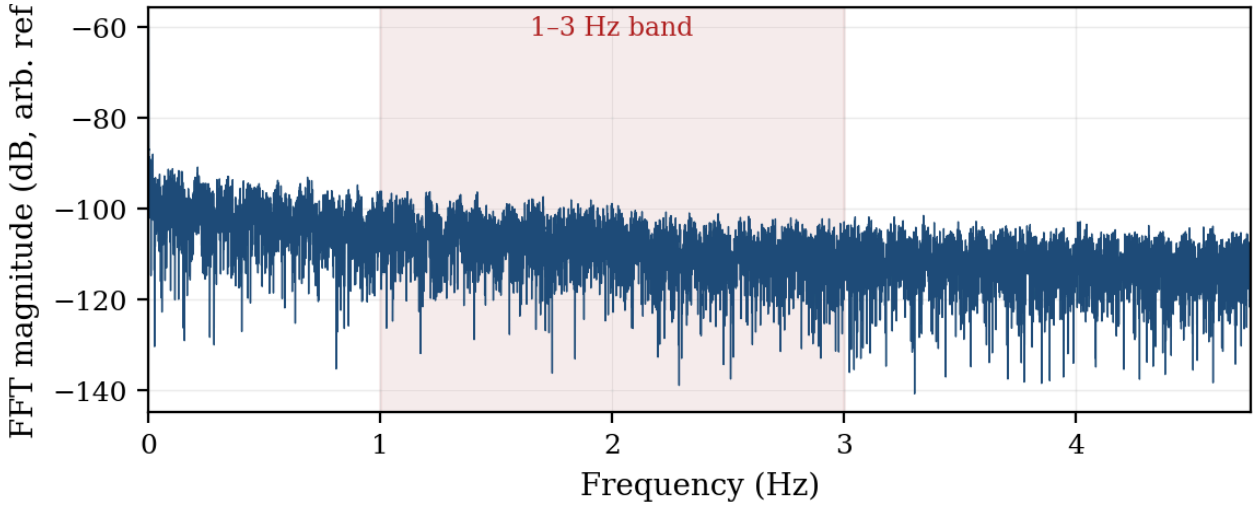


Figure 3. Magnitude spectrum of the stationary segment on a decibel scale, plotted to the 4.76 Hz Nyquist limit. Magnitude decreases with frequency across the whole range and no discrete peak is present. The shaded region marks the 1 to 3 Hz band used for event detection.

The spectrogram of the stationary segment (Figure 4) shows energy concentrated below about 2 Hz throughout, with four short intervals in which energy rises across the band.

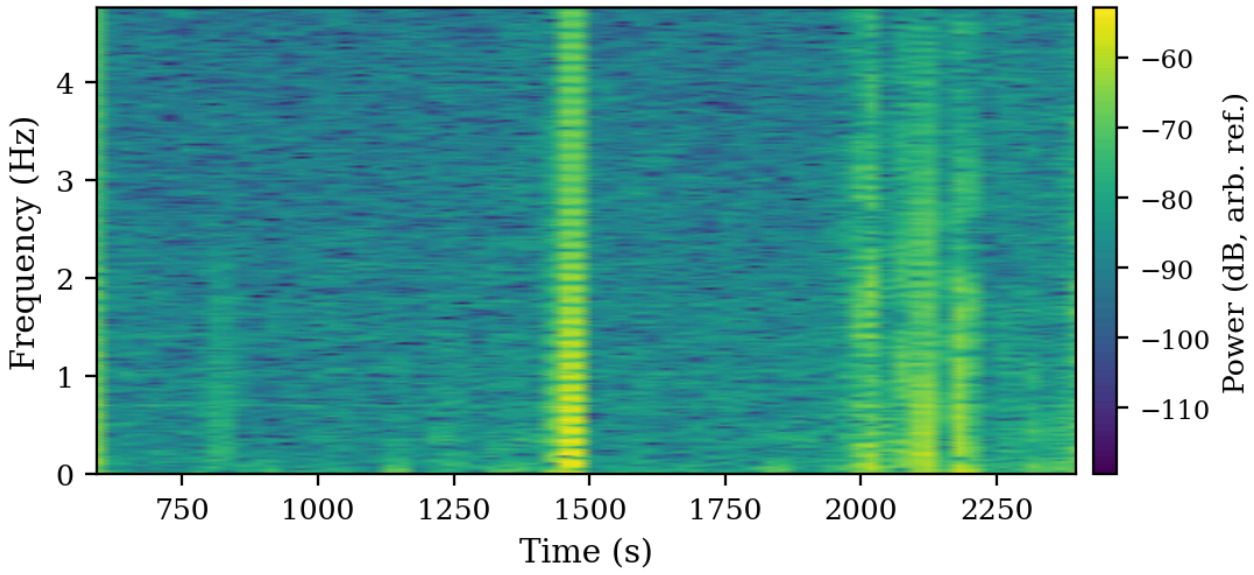


Figure 4. Spectrogram of the stationary segment. Each column spans one 53.8 s analysis window. Four vertical bands of raised energy are visible in the second half of the segment; elsewhere the pattern is uniform.

The 1 to 3 Hz band level and the four detected events are shown in Figure 5. The events fall at 1,454, 2,019, 2,127 and 2,180 s, exceeding the segment mean by 19.3, 13.4, 12.7 and 13.9 dB respectively. The interval from 565 to 1,454 s contains no detection, and neither does the final 260 s of the segment.

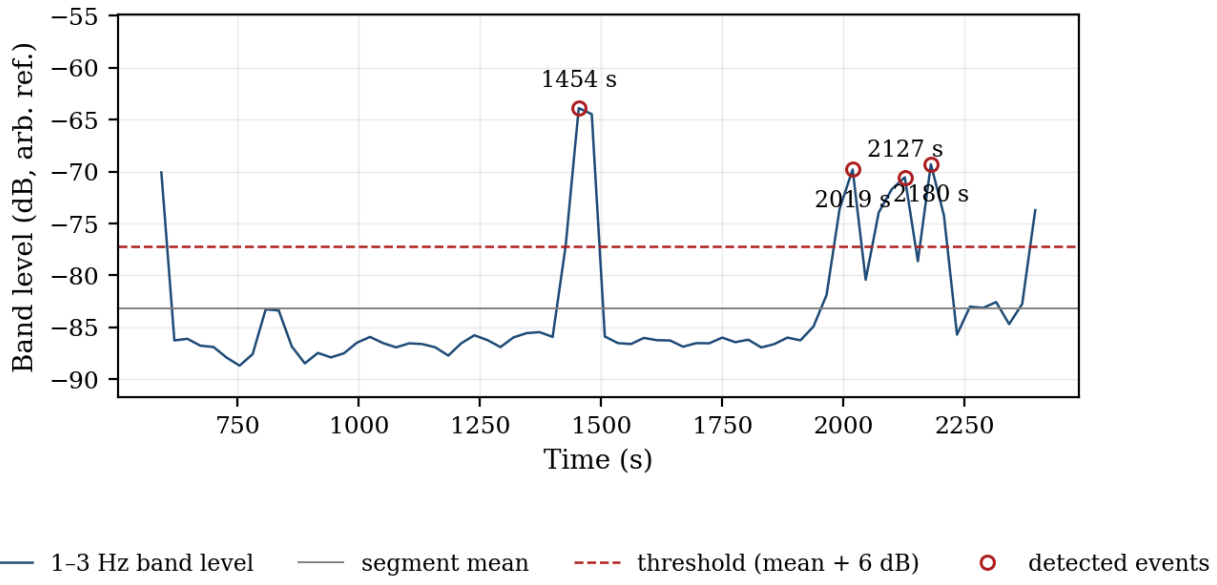


Figure 5. Mean spectrogram power in the 1 to 3 Hz band across the stationary segment. The solid line is the segment mean and the dashed line the detection threshold, 6 dB above it. Four windows exceed the threshold, marked with circles and labeled by time. The quiet interval between 565 and 1,454 s contains no detection.

Varying the analysis band and the threshold does not change the result. The same four events, and no others, are returned for every band tested between 0.5 and 4.5 Hz and for every threshold between 3 and 9 dB above the segment mean. The events are therefore broadband within the measured range rather than confined to the 1 to 3 Hz band, and the count is not a consequence of where the threshold was placed.

The surrogate test separates the events from the background more sharply still (Figure 6). Across 500 phase-randomized surrogates, each with the same power spectrum as the measured signal, the largest excursion above the segment mean was 1.9 dB and the mean largest excursion was 1.2 dB. No surrogate produced a single detection at the 6 dB threshold, or at any threshold down to 3 dB. The four measured events exceed the largest surrogate excursion by between 10.8 and 17.4 dB, so the probability that a stationary process with this spectrum produces them is below 1 in 500.

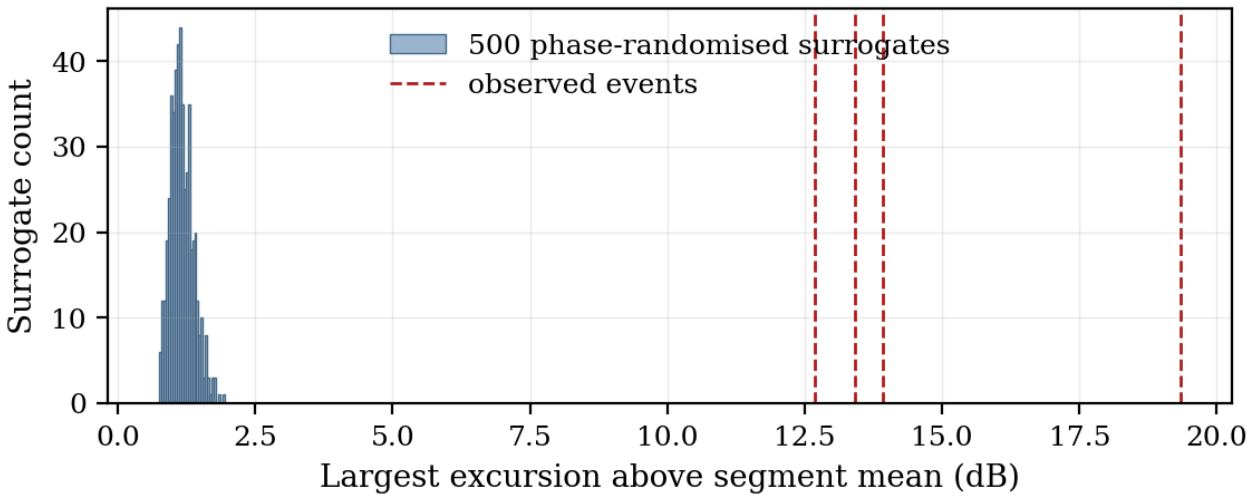


Figure 6. Distribution of the largest excursion above the segment mean in 500 phase-randomized surrogates of the stationary segment, each preserving the measured power spectrum exactly. The surrogate distribution lies between 0.6 and 1.9 dB. The dashed vertical lines mark the four measured events, at 12.7 to 19.3 dB. No surrogate produced a detection at any threshold tested.

DISCUSSION

What the Measurement Can and Cannot Reach

The meshing frequency of a gear pair is the product of the rotation rate of either gear and its own tooth count. With 100 teeth on the output gear, meshing would fall inside the measured band only if the output gear turned more slowly than one revolution every 21 s, which corresponds to an input speed below 7.1 rev/min. No motor-driven assembly runs that slowly, so the meshing frequency lies outside the measured band for any plausible operating speed, and this follows from the tooth count alone without knowing the motor. The acoustic emission associated with crack growth, which established work locates in the tens to hundreds of kilohertz (Qu et al.), lies outside the band by a far wider margin again.

What the instrument records is the slowly varying loudness of the assembly, sampled about ten times a second, so the spectrum of that record describes how quickly loudness rises and falls rather than which tones are present. Amplitude modulation of the meshing signal is the mechanism underlying established demodulation and envelope methods in gear diagnostics, in which a local fault modulates the meshing vibration once per revolution and the envelope carries the diagnostic information (Randall; Feng et al.). The present measurement reaches the low-frequency end of that same quantity, capturing an envelope while discarding the carrier that would identify its source. The spectrum of the stationary segment contains no discrete line, so no rotation rate can be identified in it, and the measurement cannot attribute an envelope fluctuation to any particular rotating component.

What the Four Events Show

The two robustness tests establish a narrow but definite result. The events are not artifacts of the analysis band or the threshold, because every combination tested returns the same four. They are not what a stationary process with this spectrum produces, because 500 surrogates built to have exactly that spectrum produced nothing above 1.9 dB while the events reach 12.7 to 19.3 dB. The recording therefore contains four genuine time-localized increases in acoustic energy, three of them within 160 s of each other near the end of the run.

What produced them is a separate question, and this study cannot answer it. At least three explanations are consistent with the observation. The gear pair may have changed, through wear or a developing surface irregularity. The two AA cells, driving a motor continuously for 42 minutes, fall in terminal voltage over that period and change the shaft speed, which moves energy across a fixed analysis band. The recording environment was uncontrolled, and a door closing or a voice nearby raises the broadband level for the duration of one window. Because no physical inspection was carried out and only one run exists, these cannot be separated. The 7.0 dB step at 565 s makes the point concretely: it is the largest single feature of the record and its cause was not noted at the time.

Relation to Established Practice

Compared with the methods used in the literature, the limits of this approach are clear. Qu et al. compared acoustic emission and vibration sensors on gearbox tooth-cut faults and found acoustic emission the more sensitive, using instrumentation operating three orders of magnitude above the bandwidth available here. Feng et al., reviewing vibration-based gear wear monitoring, describe a field built on meshing harmonics and their sidebands, none of which lie inside the band measured in this study. The relevant standard for gear units specifies broadband vibration measurement rather than a narrow low-frequency indicator (International Organization for Standardization, ISO 20816-9). The procedure demonstrated here should therefore be read as a screening indicator that flags when the acoustic behavior of a machine has changed, not as a diagnostic that identifies what changed.

The polymer literature also suggests that discrete events may be the wrong target. Mao et al., testing acetal and nylon gears, describe wear in polymer gears as a progressive process governed by contact temperature and load rather than a sequence of discrete failures, and Česnik and Slavič show that the fatigue life of additively manufactured PLA depends on loading frequency as well as stress amplitude. If polymer degradation is gradual, a slow trend in band level across many runs would be a more informative variable than isolated events within one, and a comparison of run-averaged band energy between a new gear and a worn one would test the underlying question more directly than event counting.

Limitations

Four limitations bound what is reported. The study rests on one run, so experiment-level repeatability cannot be assessed; the apparatus has been dismantled and cannot be re-run. What can be shown, and is shown above, is that the spectral description of the signal is stable to about 6 percent across four blocks of the stationary segment, which is measurement-level stability within a single record and not a substitute for repetition. No ground truth exists, since the gear was neither inspected nor sectioned afterwards, so no detected event can be associated with a physical change. The 53.8 s analysis window localizes an event only to within about half a minute. Finally, the opening 565 s of the record is excluded as non-stationary, so the method is demonstrated on 31 of the 42 minutes recorded.

Future Work

The useful next step is a better-controlled recording rather than a more elaborate analysis. A regulated supply in place of batteries would hold the shaft speed steady, and a tachometer would give the rotation rate independently, which would allow the analysis band to be centered on a known shaft frequency instead of chosen by inspection. A sampling rate high enough to reach the meshing frequency would connect the measurement to the existing literature. Repeated runs on new and deliberately worn gears, with the gear inspected between runs, would supply the ground truth this design lacks and would convert the procedure from a demonstration into a test.

CONCLUSION

This study asked whether a low-rate sound level log of a running PLA gear pair contains time-localized events that can be detected reproducibly. It does. Four events were found in the stationary 31-minute segment of a 42-minute recording, at 1,454, 2,019, 2,127 and 2,180 s, and they survive every analysis band between 0.5 and 4.5 Hz and every threshold between 3 and 9 dB above the segment mean, while 500 surrogates with the same power spectrum produced no detection at all. Because the recording is sampled at 9.51 Hz and the gear pair carries 100 and 40 teeth, the meshing frequency lies outside the measured band for any realistic motor speed, so these events are features of the acoustic envelope and not of the meshing acoustics. Whether they reflect the condition of the gear is not established here, and the single run, the absence of inspection and the uncontrolled environment each prevent it. The contribution is a reproducible detection procedure with its false-alarm behavior characterized, which is what a controlled study of gear condition would need before it began.

ACKNOWLEDGEMENTS

The author would like to thank the teachers and staff at St. Joseph's Institution International, Singapore, for their support during this project. No external funding was received for this study.

ABOUT THE AUTHOR

The student author is a high school senior in Singapore, studying the International Baccalaureate program with higher-level physics and higher-level mathematics analysis and approaches. After completing the diploma, they plan on studying engineering with a specific interest in systems for sustainability.

REFERENCES

Česnik, Martin, and Janko Slavič. "Frequency-Dependent Fatigue Properties of Additively Manufactured PLA." *Polymers*, vol. 16, no. 15, 2024, p. 2147, https://doi.org/10.3390/polym16152147.

Farah, Shady, Daniel G. Anderson, and Robert Langer. "Physical and Mechanical Properties of PLA, and Their Functions in Widespread Applications: A Comprehensive Review." *Advanced Drug Delivery Reviews*, vol. 107, 2016, pp. 367–92, https://doi.org/10.1016/j.addr.2016.06.012.

Feng, Ke, et al. "A Review of Vibration-Based Gear Wear Monitoring and Prediction Techniques." *Mechanical Systems and Signal Processing*, vol. 182, 2023, p. 109605, https://doi.org/10.1016/j.ymssp.2022.109605.

Harris, Charles R., et al. "Array Programming with NumPy." *Nature*, vol. 585, no. 7825, 2020, pp. 357–62, https://doi.org/10.1038/s41586-020-2649-2.

International Organization for Standardization. *ISO 6336-1:2019 Calculation of Load Capacity of Spur and Helical Gears, Part 1: Basic Principles, Introduction and General Influence Factors*. ISO, 2019.

International Organization for Standardization. *ISO 20816-9:2020 Mechanical Vibration, Measurement and Evaluation of Machine Vibration, Part 9: Gear Units*. ISO, 2020.

Liao, Yuhan, et al. "Effect of Porosity and Crystallinity on 3D Printed PLA Properties." *Polymers*, vol. 11, no. 9, 2019, p. 1487, https://doi.org/10.3390/polym11091487.

Mao, K., et al. "Friction and Wear Behaviour of Acetal and Nylon Gears." *Wear*, vol. 267, nos. 1–4, 2009, pp. 639–45, https://doi.org/10.1016/j.wear.2008.10.005.

Oppenheim, Alan V., and Ronald W. Schafer. *Discrete-Time Signal Processing*. 3rd ed., Pearson, 2010.

Qu, Yongzhi, et al. "Gearbox Tooth Cut Fault Diagnostics Using Acoustic Emission and Vibration Sensors: A Comparative Study." *Sensors*, vol. 14, no. 1, 2014, pp. 1372–93, https://doi.org/10.3390/s140101372.

Randall, R. B. "A New Method of Modeling Gear Faults." *Journal of Mechanical Design*, vol. 104, no. 2, 1982, pp. 259–67, https://doi.org/10.1115/1.3256334.

Sandanamsamy, L., et al. "A Comprehensive Review on Fused Deposition Modelling of Polylactic Acid." *Progress in Additive Manufacturing*, vol. 8, no. 5, 2023, pp. 775–99, https://doi.org/10.1007/s40964-022-00356-w.

Virtanen, Pauli, et al. "SciPy 1.0: Fundamental Algorithms for Scientific Computing in Python." *Nature Methods*, vol. 17, no. 3, 2020, pp. 261–72, https://doi.org/10.1038/s41592-019-0686-2.